HYDROLOGICAL PROCESSES
Hydrol. Process. **30**, 3609–3626 (2016)
Published online 22 August 2016 in Wiley Online Library
(wileyonlinelibrary.com) DOI: 10.1002/hyp.10973

Estimating runoff from a glacierized catchment using natural tracers in the semi-arid Andes cordillera

Maximiliano Rodriguez,[1] Nils Ohlanders,[2] Francesca Pellicciotti,[3] Mark W. Williams[4] and James McPhee[1,5]*

[1] *Department of Civil Engineering, Faculty of Mathematical and Physical Sciences, University of Chile, Santiago, Chile*
[2] *Geological Survey of Sweden (SGU), Uppsala, Sweden*
[3] *Northumbria University, Newcastle upon Tyne, UK*
[4] *Department of Geography, University of Colorado, Boulder, CO, USA*
[5] *Advanced Mining Technology Center (AMTC), Faculty of Mathematical and Physical Sciences, University of Chile, Santiago, Chile*

Abstract:

This paper presents a methodology for hydrograph separation in mountain watersheds, which aims at identifying flow sources among ungauged headwater sub-catchments through a combination of observed streamflow and data on natural tracers including isotope and dissolved solids. Daily summer and bi-daily spring season water samples obtained at the outlet of the Juncal River Basin in the Andes of Central Chile were analysed for all major ions as well as stable water isotopes, $\delta^{18}O$ and δD. Additionally, various samples from rain, snow, surface streams and exfiltrating subsurface water (springs) were sampled throughout the catchment. A principal component analysis was performed in order to address cross-correlation in the tracer dataset, reduce the dimensionality of the problem and uncover patterns of variability. Potential sources were identified in a two-component U-space that explains 94% of the observed tracer variability at the catchment outlet. Hydrograph separation was performed through an Informative-Bayesian model. Our results indicate that the Juncal Norte Glacier headwater sub-catchment contributed at least 50% of summer flows at the Juncal River Basin outlet during the 2011–2012 water year (a hydrologically dry period in the Region), even though it accounts for only 27% of the basin area. Our study confirms the value of combining solute and isotope information for estimating source contributions in complex hydrologic systems, and provides insights regarding experimental design in high-elevation semi-arid catchments. The findings of this study can be useful for evaluating modelling studies of the hydrological consequences of the rapid decrease in glacier cover observed in this region, by providing insights into the origin of river water in basins with little hydrometeorological information. Copyright © 2016 John Wiley & Sons, Ltd.

KEY WORDS tracer hydrology; glacier outflow; stable water isotopes; hydrograph separation

Received 1 December 2015; Accepted 19 July 2016

INTRODUCTION

The extra-tropical region of South America depends on snow and glacier melt water from the Andes Cordillera for its water supply. Although it has been well established that under future climate scenarios Andean watersheds should experience significant changes in the amount and timing of seasonal runoff (Casassa *et al*., 1998; Marengo *et al*., 2011; McPhee *et al*., 2014), the precise nature of these possible changes is still difficult to assess because of large uncertainties, including the time-varying relative contribution of snow and glacier melt as well as subsurface sources to river flow (e.g. Gordon *et al*., 2015; Ragettli *et al*., 2014). In the Andes, this problem is compounded by the difficulty in obtaining continuous time series of river discharge at close proximity to glaciers, because of the unstable nature of river beds and generally high sediment loads, remoteness of these locations and high cost of installing and operating appropriate stream gages. Without this knowledge, most hydrologic models, including those physically based, suffer from over-parameterization and can be subject to large predictive errors. In this work, we combine hydrochemical and isotopic information obtained at different locations in a semi-arid, high-elevation, moderately glaciated Andean watershed in order to discriminate among the most likely sources to the observed river hydrograph at different times during a water year. In this way, we estimate the relative contribution of a highly glacierized headwater sub-catchment where no streamflow records are available.

Hydrograph separation using natural tracers can be a useful tool to enhance hydrological conceptual and

*Correspondence to: James McPhee, Department of Civil Engineering, Faculty of Mathematical and Physical Sciences, University of Chile, Santiago, Chile.
E-mail: jmcphee@ing.uchile.cl

numerical models, through quantifying and describing the evolution of source contributions to river flow. Many hydrograph separation studies have considered chemical tracers (Heppell and Chapman, 2006; Mul *et al*., 2008), natural isotopes (Liu *et al*., 2008) or a combination of both (Ladouche *et al*., 2001; Meriano *et al*., 2011; Merot *et al*., 1995; Williams *et al*., 2006). A review of isotopic hydrograph separation was performed by Klaus and McDonnell (2013) wherein they underscore the importance of spatial variability of isotopic signals as well as on the potential for using both $\delta^{18}O$ and δD to glean deeper insights on the hydrological function of a basin. Many studies have shown the importance of soil water as a source of runoff during a rainfall event (Laudon and Slaymaker, 1997; Ogunkoya and Jenkins, 1993; Soulsby and Dunn, 2003). Other hydrograph separation studies carried out in mountainous sites have noticed the importance of snow and glacier as primary stores regulating the timing of runoff relative to precipitation occurrence (e.g. Baraer *et al*., 2009; Gordon *et al*., 2015). A description of glacier discharge and its importance as a water reservoir can be found in Jansson *et al*. (2003) and more recently in Baraer *et al*. (2012). Usually, studies of glacier mass balance present glaciological, meteorological and stream flow data to describe the glacier evolution during different seasons and under diverse climatic patterns (Hirabayashi *et al*., 2010; Kaser *et al*., 2003; Wagnon *et al*., 1999; Yu *et al*., 2013). Other studies have directly measured river flow in alpine regions where water is generated primarily because of glacier melt (Hodgkins, 1997; Mingjie *et al*., 2013; Singh *et al*., 2006), although these measurements are very difficult to sustain in time. Hydrologic models have enhanced the understanding of glacier ablation processes and their hydrological role (Hannah and Gurnell, 2001; Verbunt *et al*., 2003, among many others). Despite these efforts, large uncertainties remain with respect to the hydrologic role of glaciers in remote regions, in no small part because of the inadequate observational networks monitoring this specific aspect of the hydrologic cycle (Pellicciotti *et al*., 2014). Therefore, novel data collection techniques and interpretation tools for information of different origin/type can provide useful insights towards process understanding and improved modelling.

Snow and ice comprise the most important water sources in the semi-arid Andes, and in dry water years glacier meltwater can supply a high percentage of river runoff during the dry, warm months of the austral summer (DJF). Efforts have been made in the past to better describe the contribution from snow- and glacier melt to streamflow in Andean basins (Gascoin *et al*., 2011; Pellicciotti *et al*., 2008; Peña and Nazarala, 1987; Ragettli and Pellicciotti, 2012). These works estimate variable glacier contribution depending on climatic factors, with increasing relative contribution in dry years, but are affected by the scarcity of glacier runoff observations. Ohlanders *et al*. (2013) used a simple mixing model with two components to attempt an estimation of the contribution from glacier melt and snowmelt sources to river flow during the 2011/2012 water year at the Juncal River Basin, an alpine river catchment in central Chile. A large degree of uncertainty affected those results, stemming from a very similar isotopic signature between runoff from glaciated areas and that of runoff from high-elevation, non-glaciated areas.

In this study, we build upon the work by Ohlanders *et al*. (2013), who document the contribution of different sources to river flow using isotopic data measured in different sections of the river, in the snowpack, and rainfall. Now, we complement that study by incorporating solute data recorded during the same period, quantifying as well the uncertainty of the estimated runoff contributions. Specifically, we aim to: (i) discuss the information content of natural tracer observations with respect to mountain river flow, (ii) demonstrate a methodology for spatial hydrograph separation in Andean watersheds in order to identify the relative contributions of ungauged sub-basins to a monitored catchment, and (iii) focus on the contribution from a glacierized headwater sub-catchment to streamflow in order to highlight the importance of ice masses in regulating and sustaining hydrological systems during periods of drought.

In this work we use an Informative-Bayesian Mixing model, which yields probabilistic distributions of the relative contribution of each source to river flow. Bayesian models have been used in several types of mixing problems, especially in ecological research settings (Parnell *et al*., 2010; Semmens *et al*., 2009), and also in hydrological applications (e.g. Freer *et al*., 1996; Liu and Gupta, 2007; Wikle and Berliner, 2007). In the context of hydrograph separation, Cable *et al*. (2011) documented source contributions on a glaciated basin using a non-informative hierarchical Bayesian model. Our approach incorporates the knowledge acquired in past studies to the model and updates the probability density functions of relative contributions as new data becomes available.

STUDY AREA AND AVAILABLE DATA

Study area

The Juncal River Basin (with outlet at Junc-R1) is located in the Andes of central Chile, 60 km to the northeast of Santiago, Chile's capital city (Figure 1). It is a 236.2-km^2 mountain catchment with an elevation range of 2200 – 6100 m a.s.l. and an area-averaged elevation of 3500 m a.s.l. approximately. In its headwaters, the basin

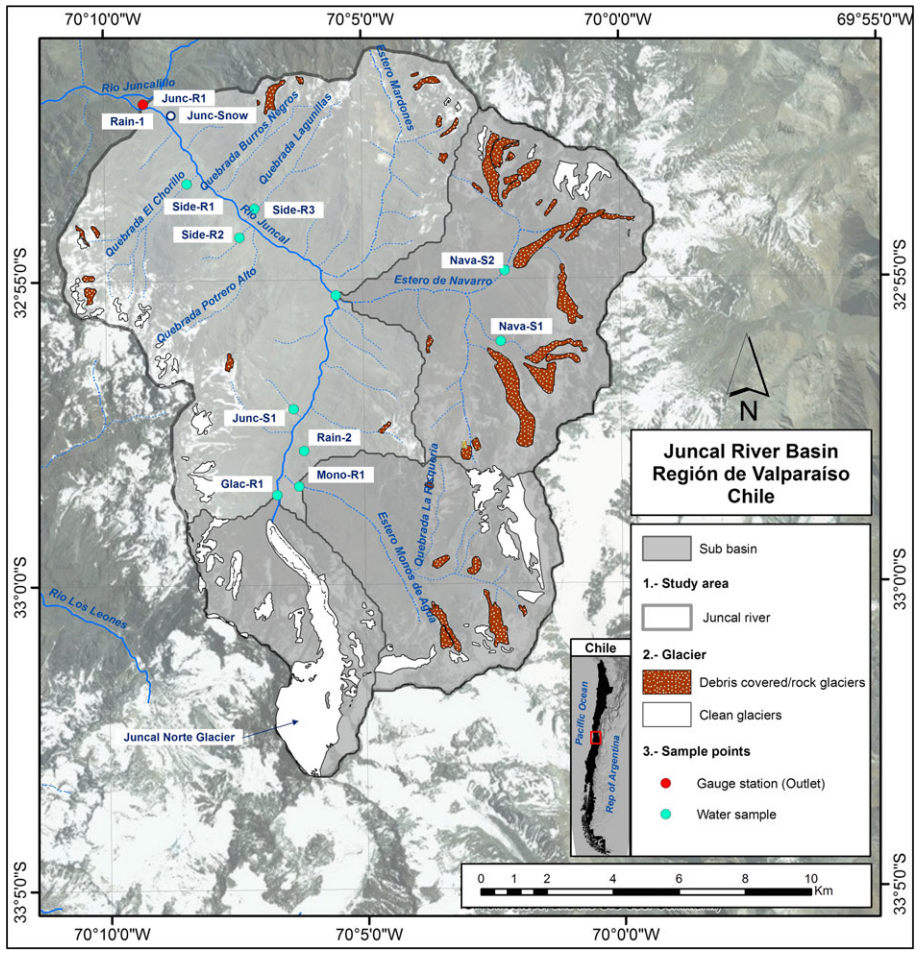

Figure 1. Study site. Sub-catchments, the Juncal Norte Glacier, rock glaciers within the basin and sampling points are depicted. Inset maps show the region's location within Chile's territory (large) and basin general location within the Valparaíso Region (small)

holds a total of 71 glaciers of varying size, which cover a total of 47 km^2, or 19% of the catchment area (Bown *et al*., 2008). Of these, clean or bare-ice glaciers cover 35 km^2, while debris-covered and rock glaciers cover 12 km^2. Clean glaciers concentrate in two areas in the southern part of the Basin, here referred to as the Juncal Norte Glacier (Glac-R1) and the Mono de Agua (Mono-R1) sub-catchments, while debris-covered glaciers exist primarily in the Navarro Creek (Nava-R1) sub-catchment. Of the clean glaciers, the Juncal Norte has drawn increased attention from the scientific community in recent years, in part because of its size and its accessibility compared to other ice bodies in the region. Bown *et al*. (2008) report a 1.46 km^2 area loss at the Juncal Norte Glacier for the period 1955–2006 based on satellite image analysis, which is equivalent to an average 9.1-m annual frontal reduction rate over the same period. No long-term mass balance data exist for the Juncal Norte or other glaciers in the basin, but Pellicciotti *et al*. (2008) report cumulative ablation rates of up to 4000 mm water equivalent (w.eq.) over two months during the austral summer of 2005/2006. The climate in the region is semi-arid with cold winters and warm, dry summers. The mean annual temperature in 2011 at the Junc-R1 outlet (located at 2200 m a.s.l.) was 9.9 °C. Annual precipitation is about 600 mm at an elevation of approximately 3000 m a.s.l. (Dirección Meteorológica de Chile Publications, 2001) and, coherently with the Mediterranean characteristics of the local climate, is heavily concentrated in the winter months of June through August, with at least 75% of the annual precipitation average occurring within this period of the year. At this latitude, wintertime precipitation occurs mainly in solid phase above 1600 m a.s.l. Spring melt starts at the beginning of September, and for the study area most of the snow cover as retrieved by the Terra/MODIS MOD10A product disappears by late November, with the exceptions of isolated pockets of shaded or high elevation sites which overlap with the accumulation zone of existing glaciers (Ohlanders *et al*., 2013; Ragettli *et al*., 2014).

The geology of the eastern part of the basin is dominated by limestone and calcareous sandstone, which are easily

weathered, influencing the chemistry of the river and resulting in very high concentrations of calcium ions. These coexist with igneous formations that provide the water with a distinct, high sulphate concentration. In some areas in the northeastern reaches, natural gypsum deposits have been identified and exploited commercially. Volcano-sedimentary strata dominate the local lithology in the central and western parts of the basin, with an important presence of dacitic, pyroclastic and basaltic rocks.

The basin is vegetated predominantly with camaephytes species, which grow at the lower edge of talus formations along the river valley. In the upper portion of the watershed, mountain bogs cover valley bottoms, whereas a more defined floodplain develops in the lower portion of the basin, where phanerophyte vegetation can be found. No formal soil data was obtained for this study, but from road cuts it can be seen that soils can develop up to 2–3 m in depth, with little organic content but with high fine fractions outside of the aforementioned talus formations, which consist mostly of loosely packed gravel material.

Hydrometeorological data

Streamflow data are available at the 'Juncal at Juncal' stream gauge, which demarcates the outlet of the Junc-R1 basin and is operated by the Chilean Water Directorate (Dirección General de Aguas, DGA). This stream gauge has been active since 1970, its rating curves are updated regularly and records hourly data. Historical monthly flows range between 1.0 and 30.0 $m^3 s^{-1}$, with an annual mean flow of 6.2 $m^3 s^{-1}$, equivalent to a specific annual discharge of 764 mm.

Air temperature, radiation and precipitation are measured at two meteorological stations in the vicinity of the basin, namely 'Hornitos' and 'Riecillos'. The former is operated by the Department of Civil Engineering at Universidad de Chile, and is located in the outlet of the catchment; the latter is operated by DGA and is located approximately 20 km west from the catchment outlet, at an elevation of approximately 1250 m a.s.l. Riecillos is the nearest operational weather station to the study area and has a longer period of record of precipitation and air temperature (1929 – 2015). Mean annual precipitation at the Riecillos station is 510 mm, and average temperature is 8.9 °C.

Water isotope and chemical data

DGA has recorded river flow solute data at the catchment outlet since 1996, reporting concentrations of major metals (Cu, Ag, Al, Mg, Ca, etc.), nonmetals (Cl, inorganic N and P, etc.) and some water quality parameters like temperature and pH, for samples obtained every three or four months approximately.

Our team carried out fieldwork campaigns between January 2011 and April 2012 in order to sample water characteristics in various-sized streams within the basin, as well as in rain and in the seasonal snowpack (Figure 1). Water samples at the Junc-R1 outlet were collected manually every two weeks approximately for the first half of the study period (winter season). In early October 2011, an automatic sample collector was installed at this location. From then until the end of the study period, samples were obtained at two-day (early spring) or one-day (on late spring and early summer) intervals, always at 17:00 LT. Other sampling sites where selected in order to characterize waters from different spatial sources within the main basin. These include streamflow at the Juncal Norte Glacier snout (Glac-R1), the outlets of the Navarro and Mono de Agua creeks (Nava-R1 and Mono-R1, respectively) and surface waters sampled at streams flowing from western and eastern slopes along the main river channel (Side-R1, 2 and 3, respectively). Glac-R1 water samples were obtained less than 100 m downstream from the glacier terminus, with no other visible sources of flow between the glacier snout and the sampling site. The eight available samples were obtained in seven different months between April 2011 and April 2012, with the majority (seven) of them corresponding to the melt season between September 2011 and April 2012. The lack of available groundwater sampling sites motivated the sampling of spring waters seeping into the river channel at different locations within each tributary to the Juncal River. These included Mono de Agua (Mono-S1, Mono-S2 and Mono-S3), Navarro (Nava-S1 and Nava-S2) and a spring near de Juncal River main Channel (Junc-S1). Figure 1 shows that the Nava-S1 and Nava-S2 sampling sites are located very close to the terminus of rock glaciers. Two rain collectors were set up in the Juncal basin (the first at the Junc-R1 outlet – Rain-1 – and the second near the Juncal Norte glacier – Rain-2), while a third was located in a location outside the catchment, at an elevation of 2099 m a.s.l. These rain collectors were deployed at intervals between September 2011 and April 2012, and as such sampled mostly liquid-phase spring and summer precipitation. Snowpack samples were collected by sinking polyvinyl chloride (PVC) tubes through the entire depth of the snowpack. A first set of samples were obtained along a nearby mountain road during one day in late winter ('Snow-road'; August 10, 2011), in order to study the altitudinal gradient in snow isotopic composition in the range 2200–3000 m a.s.l., as reported by Ohlanders *et al.* (2013). Also, several snow samples were collected near the Juncal River outlet ('Snow-Junc'; 2200 m a.s.l.) during the winter season of 2011. Some samples were collected before beginning of snowmelt (between 4 and 21 August 2011), while two additional samples were obtained one and two weeks after

snowmelt began (13 and 21 September 2011). Snow samples were preserved in plastic bags stored in cooler boxes filled with ice during transport to the lab. Once in the lab, they were stored at 4 °C and allowed to melt at that temperature. Resource availability and accessibility constraints prevented us from obtaining frequent snowmelt samples for isotopic and chemical analysis. Only two melt samples – 'snow-melt' – were obtained on 13 and 21 September 2011 (beginning of the melt season). In the absence of snow lysimeters, these samples were obtained by digging snow pits, sliding polypropylene sheets under the snowpack and funneling the melt to sample bottles (Williams and Melack, 1991). Each snowmelt sample was collected over the course of a few hours. No melt samples were obtained in subsequent months because of the rapid snow cover retreat during the 2011 season, which prevented our team from safely reaching sites with relevant snow depths within the basin.

METHODOLOGY

Laboratory analysis

All manually obtained water samples were filtered on site at the time of collection using a 0.45-μm nitrocellulose filter (Type HAWP04700) in order to prevent the possible dissolution of minerals present in suspended solids inside the sampling bottle prior to laboratory analysis. After filtration, water for cation analysis was acidified with nitric acid at 4 N to avoid mineral precipitation and was stored in high-density plastic bottles. Samples for anion analysis were preserved at 5 °C in the laboratory. Samples from the automatic collector were filtered at the moment of retrieval, approximately every two weeks. Same-day samples from the automatic collector and manual samples from field campaigns were compared to characterize the potential bias introduced by the delayed filtering of automatically collected samples. Alkalinity was measured through Titration at the Water Quality Lab at the Department of Civil Engineering and at the Geochemistry Lab at the Geology Department, Universidad of Chile, following the procedures described by Neal (2001). Water samples were analysed for SO_4^-, Cl^-, Ca^{2+}, K^+, Mg^{2+}, Na^+, Si, as well as for stable water isotopes δD and $\delta^{18}O$, following a methodology similar as that proposed by Barthold *et al.* (2011). Bicarbonate concentrations were impossible to obtain from automatic samples because of the two-week delay between sampling and lab analysis. However, we verified the quality of our automatic samples by replacing the missing bicarbonate values with estimates from a set of manual samples obtained throughout the season at the same hour and location as those of the automatic sampler. In all cases, manual samples obtained at Junc-R1 were balanced. Furthermore, ion concentrations in these manual samples where indistinguishable from those from the automatic samples (except for bicarbonate, evidently). Samples obtained at other locations sometimes displayed a slight ionic imbalance, and those with charge balances greater than ±10% were discarded from the remaining analyses. Major cations as well as Si were measured by an Inductively Coupled Plasma-Optical Emission Spectrometer (ICP-OES, Optima 7300 V, HF version) at the Geochemistry Lab at the Geology Department at University of Chile and by an Inductively Coupled Plasma Atomic Absorption Spectrometer (ICP-AES, Perkin Elmer Optima 3000) at the Research Analytical Laboratory at University of Minnesota. Detection limits for cations are 0.01 mg/lt, and precision ranges between 2.4 (Ca^{2+}) and 0.2 (Mg^{2+}) mg/lt. Anion concentrations were measured by an ion chromatographer (861 advanced compact) at the University of Chile and by an ion chromatographer (Dionex model DX-120) at the University of Minnesota. Detection limits for anions are 0.002 mg/lt, and precision ranges between 0.3 and 0.5 mg/lt. Samples were sent to the Ehleringer Lab, at the University of Utah, for stable isotope analysis. Isotope values have a precision of $0.2^{\circ}/_{oo}$ for $\delta^{18}O$ and $2.0^{\circ}/_{oo}$ for δD.

Hydrograph separation

A Bayesian framework was established in order to explicitly account for measurement, model and parameter uncertainty by estimating the probability density function of each source's contribution to flow. Compared with deterministic methods such as end member mixing analysis (Christophersen *et al.*, 1990; Christophersen and Hooper, 1992), the Bayesian approach also enables estimates of the uncertainty bounds on the percentage contribution of each source, and as such provides information useful for characterizing possible weaknesses as well as for guiding data collection strategies for improving the mixing model. Equations 1, 2 and 3 describe the Bayesian model.

$$p(\mathbf{f}_q|data) = \frac{p(data|\mathbf{f}_q)\times p(\mathbf{f}_q)}{\sum p(data|\mathbf{f_q})\times p(\mathbf{f_q})} \quad (1)$$

$$0 \le \mathbf{f}_q \le 1 \quad (2)$$

$$\sum_i f_{q,i} = 1 \quad (3)$$

The vector $\mathbf{f}_q$ contains the source contribution in each component, and subscript q indicates the q-th realization of a random process. The probability $p(\mathbf{f}_q)$ represents the prior distribution, and $p(data|\mathbf{f}_q)$ is the likelihood function

of observed data given a state of nature ($\mathbf{f}_q$). The denominator is a numerical approximation of the marginal probability, necessary for normalizing the posterior probability $p(\mathbf{f}_q|data)$. Prior information takes the form of candidate probability distributions for each random variable. The prior distributions need not capture precisely the true behaviour of each variable, but instead are expected to give a wide enough range of uncertainty, informed by the best understanding of the possible range of behaviour of the system. In principle, prior distributions may be 'non-informative', in the sense that they should not introduce bias to the analysis, although informative priors can be employed when granted by knowledge about the system. Several possible distribution shapes may be adopted as priors, and here we adopt a Dirichlet distribution, which is usually utilized in Bayesian analysis when multiple variables adopting values in the 0–1 range are studied. The form of the Dirichlet prior is:

$$\mathrm{P}(\mathbf{f}) = \mathrm{Dir}(\alpha) = \frac{\Gamma(\alpha_1 + \ldots + \alpha_\mathrm{k})}{\Gamma(\alpha_1)\cdot\ldots\cdot\Gamma(\alpha_\mathrm{k})}\cdot f_1^{\alpha_1-1}\cdot\ldots\cdot f_k^{\alpha_k-1} \quad (4)$$

where

$$\sum_{\mathrm{i}=1}^{\mathrm{k}} \mathrm{f_i} = 1\,;\, \mathrm{f}_1, \ldots, \mathrm{f_k} \geq 0. \quad (5)$$

Based on previous experience at the basin and having no data to suggest otherwise, we adopted initial values of 1.33 for all α_i, which translates in a probability peak at a contribution of 1/3 for each source.

The likelihood function represents the probability of observing the data measurements given some values of the distribution parameters. We defined the likelihood as a multivariate normal distribution, whose dimension depends on the number of tracers selected. The limited number of samples obtained from each source does not allow determining if the data behave normally. However, the Jarque–Bera test (Thadewald and Büning, 2007) was performed in order to verify the normality (with unknown mean and variance) of each source samples. The results show that there is not enough evidence to reject the null hypothesis in all samples with exception of isotopic samples obtained at the Mono-R1 site. Nevertheless, given the small number of samples at this site and the difficulty in assigning a different distribution, together with the lack of evidence of a trend in the observed values, we assign the same distribution to these samples as to the rest of the observations obtained throughout the study area and period.

The proposed mean and variance were computed from random values of f_i (Moore and Semmens, 2008), under the assumption that the mean of the mixture is a linear combination of the mean of the sources, and that the variance is quadratically proportional to the variances of the sources (Equations 5 and 6). We used a simple Bayesian model because given the origin of the available data it is difficult to assign a well-suited probability density function to hyper parameters. Therefore, the mean and variance of each source in our analysis were directly set from the values measured. As mentioned before, the mean and standard deviation of the posterior distributions for each source are obtained with,

$$\hat{u_j} = \sum_{i=1}^{n} f_i \times m_j^i \quad (5)$$

$$\hat{\sigma_j} = \sqrt{\sum_{i=1}^{n} {f_i}^2 \times \left(S_j^i\right)^2} \quad (6)$$

were m_j^i and S_j^i are the mean and standard deviation of the jth tracer on the ith source, respectively.

Because of the complexity of the analytical solution of Equation 1, we applied a Markov Chain Monte Carlo (MCMC) algorithm in order to find a numerical solution to the Bayesian model based on random values of f_i. We adopted a block-wise updating procedure, which is equivalent to a generalized multivariate approach of the Metropolis–Hastings sampling algorithm (Steyvers, 2011). For each day, 5000 random values of f_i were generated in order to draw the posterior distribution. The i-th source contribution was estimated as the weighted mean of the 5000 f_i given the value of the likelihood function in each case.

RESULTS AND DISCUSSION

Stream water chemistry and isotopic composition

Table I shows a summary of all sample solute concentrations and isotopic signatures obtained during the 2011/2012 water year in our study area. The last three rows correspond to snow core samples obtained along a road in the vicinity of the basin (Snow-road; 2000 – 3000 m. asl.), to snow cores sampled at the basin outlet (Snow-Junc; 2200 m. asl.), and to snowmelt obtained at the Snow-Junc site (Melt-Junc; 2200 m. asl.), respectively. Standard deviations are shown in parenthesis.

Figure 2 shows the temporal evolution of several variables observed at the Juncal River Basin outlet (Junc-R1). River flow values are daily averages from hourly data as recorded by the gauging station, and air temperature values are those measured at the Hornitos station, located at the basin outlet. Stable isotope and solute values correspond to manual samples collected every two weeks on average before 1 October, and

Table I. Summary statistics of all solute and isotope measurements. Each row shows the mean and standard deviation (in parenthesis) of all available observations.

Site	Elev [m a.s.l.]	N	Begin date	End date	Cl^- [mg/l]	SO_4^{-2} [mg/l]	Ca+2 [mg/l]	Na+ [mg/l]	Mg+ [mg/l]	K+ [mg/l]	Si [mg/l]	HCO^{3-} [mg/l]	δ D [‰]	$\delta^{18}O$ [‰]
Junc-R1	2250	121	07-12-2010	21-04-2012	10.6 (6.3)	243.4 (88)	103.1 (32.3)	9 (3.6)	8.3 (2.7)	1.4 (0.4)	2.6 (0.6)	95.1 (12.3)	−127.3 (1.7)	−17.3 (0.3)
Glac-R1	2900	8	30-04-2011	03-04-2012	3.3 (2.9)	33.5 (15)	24.1 (7.8)	3 (1.6)	3.5 (0.7)	0.8 (0.4)	1.9 (2.7)	45.8 (15.3)	−130.7 (2.7)	−17.9 (0.4)
Nava-R1	2460	7	23-03-2011	23-04-2012	18.7 (6.3)	817.2 (28)	286.9 (25.4)	15.6 (1.7)*	13.5 (1)	2.7 (0.4)	4.5 (0.4)	110.3 (5,3)	−127 (1.1)	−17.2 (0.2)
Rain-2		3	06-09-2011	05-12-2012	3.5 (2)	4.1 (1.6)	6.7 (4.2)	1.8 (0.7)	0.6 (0.1)	0.3 (0.4)	0.4 (0.4)	-**	−81.5 (67.8)	−11.6 (8.7)
Side-R3	2346	2	29-11-2011	12-03-2012	22.9 (4.9)	17.2 (17)	22.7 (15.5)	6.7 (7.6)	2.2 (1.3)	0.2 (0.2)	3.5 (0.6)	63.9 (0)	−113.8 (3.4)	−15.2 (0.9)
Mard R1	2470	1	04-04-2012	04-04-2012	33.2 --	277.7 --	107.3 --	-**	14.5 --	1.9 --	4.4 -	-**	−122.2 --	−16.5 --
Nava S2	3050	1	24-04-2012	24-04-2012	9.1 --	994.8 --	346.2 --	-**	16.3 --	3.9 --	5.3 --	149.2 --	−128.8 --	−17.6 --
Nava S1	2900	1	24-04-2012	24-04-2012	9.6 --	1125.9 --	388.2 --	18.2 --	15.2 --	5.8 --	6 --	136.4 --	−127.4 --	−17.3 --
Mono S1	3200	1	03-04-2012	03-04-2012	20.4 --	885.4 --	299 --	-**	19.4 --	6.5 --	3.7 --	82.1 --	−135.3 --	−18.2 --
Mono S2	2950	1	03-04-2012	03-04-2012	21.2 --	320 --	118.7 --	-**	9.3 --	2.4 --	3.4 --	57.8--	−132.4 --	−17.7 --
Mono S3	3280	1	03-04-2012	03-04-2012	15.5 --	201 --	80.8 --	-**	6.5 --	1.4 --	3.1 --	62.6 --	−131.1 --	−17.5 --
Junc-S1	2745	3	24-01-2012	02-04-2012	25.8 (27)	418.1 (22.6)	172.5 (32.7)	10.5 (1.4)	15.5 (3)	3.1 (0.1)	3.6 (0.6)	87.0 (3.2)	−132.4 (2.4)	−17.9 (0.2)
Side-R2	2680	1	12-03-2012	12-03-2012	0.6 --	45.4 --	53.9 --	6.6 --	14.5--	0.8 --	3.0 --	105.3 --	−115.9 --	−15.7 --
Side-R1	2379	2	29-11-2011	25-01-2012	0.9 (0)	20.8 (7.9)	20.4 (4.7)	2.5 (0.6)	4 (0.9)	0.3 (0.1)	2.0 (0.3)	54.1 (20.7)	−112 (1.5)	−15.3 (0.5)
Mono-R1	2800	6	30-04-2011	04-12-2012	11 (4.9)	550.3 (150.2)	191.9 (51)	12.6 (3.4)	16.4 (4.4)	2.8 (0.7)	3.2 (0.8)	79.7 (16.7)	−136 (1.8)	−18.3 (0.3)
Snow-road	2200 – 3000	10	10-08-2011	10-08-2011	2.33 (1.87)	1.01 (0.25)	2.38 (5.48)	1.43 (1.57)	0.34 (0.52)	0.31 (0.04)	0.10 (0.07)	NAN	−128.29 (12.56)	−17.23 (1.56)
Snow-Junc	2250	13	04-08-2011	21-09-2011	0.68 (0.28)	0.97 (0.46)	0.53 (0.28)	0.24 (0.11)	0.20 (0.08)	0.42 (0.42)	0.06 (0.00)	NAN	−109.13 (4.84)	−15.01 (0.74)
Melt-Junc	2250	2	13-09-2011	21-09-2011	1.17 (0.35)	0.73 (0.06)	0.83 (0.26)	0.72 (0.30)	0.18 (0.00)	1.02 (0.00)	0.06 (0.00)	NAN	−101.00 (1.64)	−13.46 (0.25)

Note:
*Only five available samples because of missing data.
**No data available.

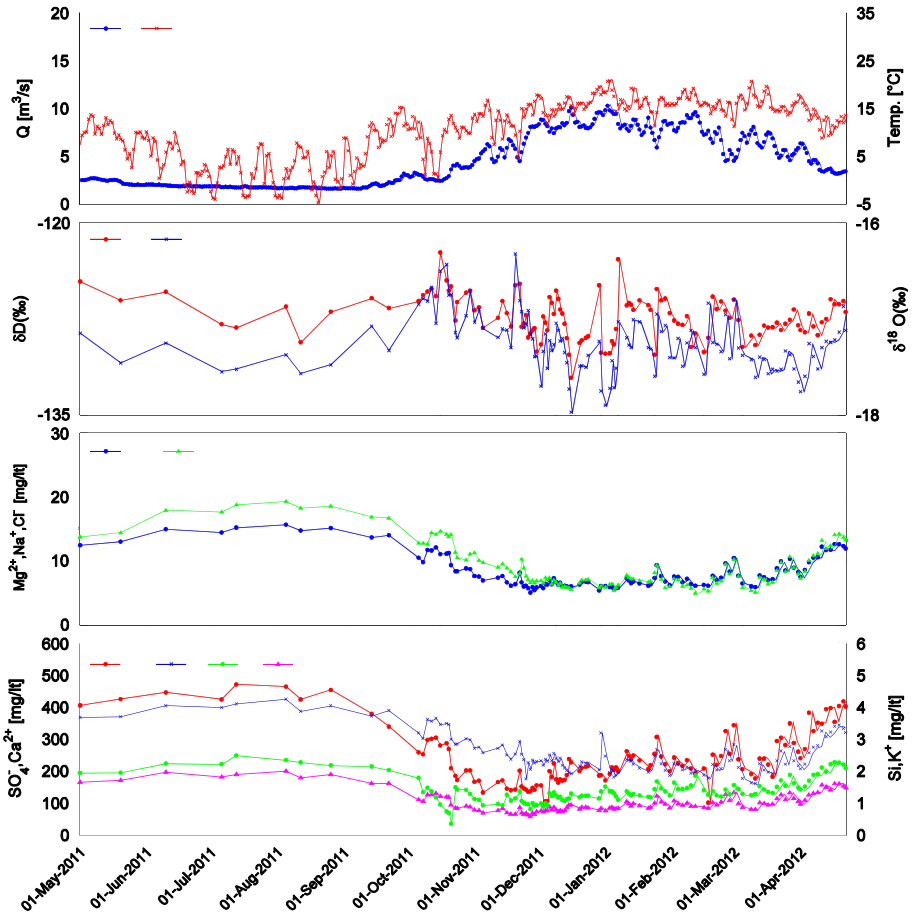

Figure 2. Time series of recorded datasets at the Juncal River Basin outlet: A) daily river flow, B) stable water isotope signature, C) and D) dissolved ions

automatic samples obtained every two days afterwards. Three periods may be identified from inspection of the time series. The first, spanning from May 2011 to mid October 2011, corresponds to late fall through early spring. Here we observe a very stable river flow in the order of 2.5 $m^3 s^{-1}$, with a slight decreasing trend. A first streamflow pulse occurs at the very end of this period, followed by a discernible pulse in isotopic signal (towards more enriched water) as well as pulses in solute concentrations, except for K, around 15 October. Most likely, this pattern can be explained by the 'old water paradox' pointed out by Kirchner (2003), where a melt pulse flushes water that has resided longer in the basin. The effect of different elevations contributing to snowmelt and runoff can be seen in the quickly falling $\delta^{18}O$ and δD values during October and November (Figure 2b), where higher-elevation areas contribute to stream water until no snow remains in the catchment (see also Ohlanders *et al.* (2013)). This spatial difference in isotopic composition dominates the dynamics of how snowmelt affects stream water isotopes and must therefore be accounted for, while the effect of elution and isotopic fractionation during melt, which is very important in catchments with little differences in elevation, probably had a more limited effect here (Liu *et al.*, 2004; Williams *et al.*, 2009).

The second period spans from mid October 2011 to late December 2011, and the seasonal hydrograph shows a rising limb towards high flows in the order of 10 m^3/s. This period is characterized by flow variability and by a decreasing trend in solute concentrations as well as a trend towards more depleted isotopic characteristics (but with very high variability). The last period spans from December 2011 to April 2012, after flow has peaked, and decreases towards the winter baseflow levels observed between May and October 2011. At the same time, ion concentrations increase towards the high concentrations observed in the winter of 2011. By the end of the water year, solute concentrations show values comparable to those observed at the beginning of the study period, although river flow on April 2012 is higher than what was recorded in early May 2011.

Figure 3 displays the spatial variability in observed solute concentrations in water samples throughout the

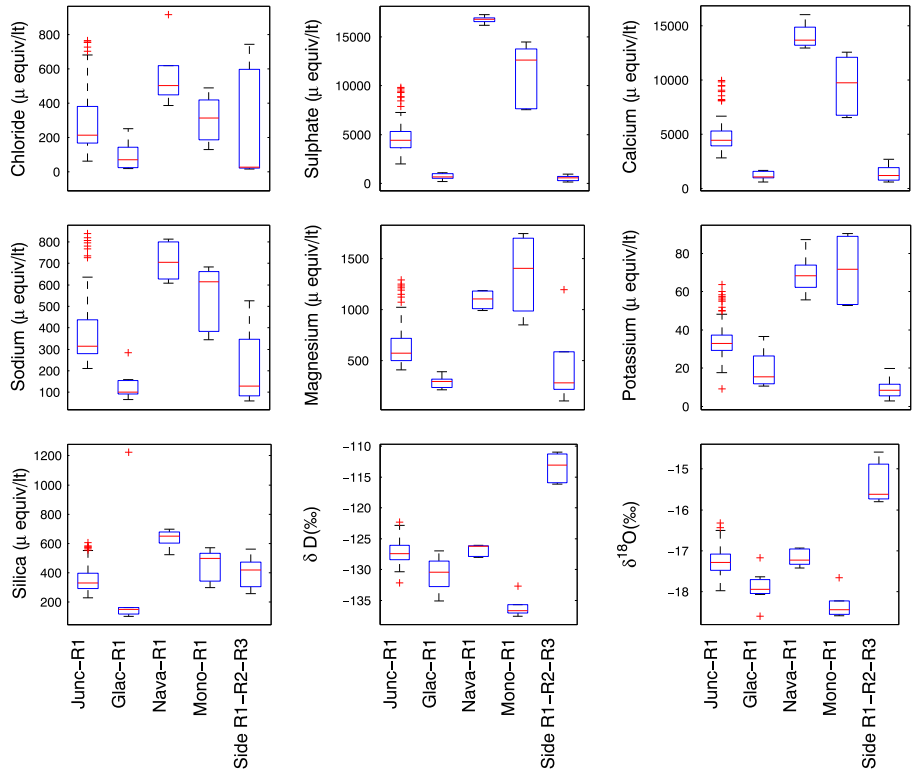

Figure 3. Spatial distribution of solute data. Boxes indicate first and third quartiles. Red line indicates the median of observed values. Whiskers are maximum and minimum values after outliers (red crosses) were removed

basin, and detailed numerical values are shown in Table I. The most salient feature observed from solute data is the high SO_4^- and Ca^{2+} concentrations at the basin outlet (Junc-R1), which are related to the even higher concentrations obtained at the interior sampling locations Nava-R1 and Mono-R1. High SO_4^- and Ca^{2+} concentrations originate principally by interaction between water and the soil matrix in conjunction with the local geology, which does show a marked preponderance for sulphate-calcium facies towards the east of the valley bottom (SERNAGEOMIN, 2002). The high solute concentration in these samples matches very closely that of individual samples obtained at springs flowing near the toe of rock glaciers towards the end of the study period (Nava-S1 and Nava-S2, see Table I). Samples obtained from the western slopes along the valley bottom (Side-R1, R2 and R3) show lower concentrations in almost all solutes, suggesting a shorter contact time between the soil matrix and water coming from this area. Glac-R1 samples show very low solute concentrations, among the lowest of all water samples obtained in streams. These samples integrate hydrological processes occurring throughout the contributing area to the sampling point, which includes on-glacier and off-glacier sites. However, the Juncal Norte glacier covers approximately 33% of the surface area of the contributing sub-basin to the Glac-R1 site. The rest of the area is dominated by steep slopes (Ragettli *et al.*, 2014) such that a fair amount of snow redistribution could be expected to happen towards the glacier surface. No observed estimates exist, unfortunately, and this is a source of uncertainty that must be addressed in future research. Last, ion concentrations measured in the snow samples are, as expected, much lower than those measured at stream sites. Nevertheless, Cl^- shows significant concentrations in the snowpack, but with a high degree of variability as suggested by the difference between Snow-road and Snow-Junc sites (Table I). Snowmelt samples were enriched in some solutes with respect to bulk snow samples, particularly in Cl^-, Na^+ and K^+. The enrichment factor varied from approximately 1.0 to 3.0, which is in the order of, but somewhat lower than, values reported in snowmelt studies in other regions (Johannessen and Henriksen, 1978; Williams and Melack, 1991). The limited number of samples taken in our study, and the fact that snow core samples were analysed without phase separation, prevent us from analysing this result in depth.

Isotopic composition of snow, snowmelt and interior stream samples

Figure 4 depicts the δD–$\delta^{18}O$ plot for snowpack ($n = 23$) and stream ($n = 128$) water samples taken in the area during the period of study. Included are snow core samples taken

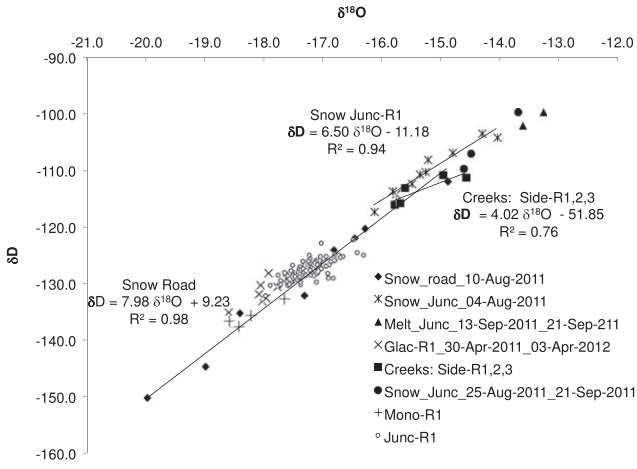

Figure 4. Stable water isotope characteristics of snow and snowmelt samples. 'Snow Road' samples were obtained along route 60, within the 2500 – 3000 m a.s.l. elevation band. 'Snow Junc' samples are snowpack samples obtained in the vicinity Junc-R1 site. Number code beside each symbol in the legend corresponds to the date the samples were obtained (dd-mmm-yyyy)

along the Chile–Argentina international road at the beginning of August 2011 as described in Ohlanders *et al*. (2013) (black diamonds) and snow core samples obtained in the vicinity of the basin outlet between 4 August 2011 and 21 September 2011 (asterisks and black circles depending on the date). Additionally, the figure shows the isotopic composition of the proglacial stream close to the snout of the Juncal Norte glacier (Glac-R1, crosses); the stream draining the 'Mono' glacial headwater (Mono-R1), as well as five stream water samples obtained at the Side-R1, 2 and 3 sites (black squares). Variation in $\delta^{18}O$ among road snow samples is comparatively large (between −19.97 and −14.9‰) and is a function of elevation, as shown by Ohlanders *et al*. (2013). The slope of this line is 7.98, which is indistinguishable from the GMWL, ($\delta D = 8.13 * \delta^{18}O + 10.8$) (Craig, 1961), suggesting that the snow pack at these sites suffered little or no isotopic fractionation during the winter season. During fieldwork at these sites, almost no liquid water was observed, which reinforces this idea. In contrast, the snow core samples obtained at the basin outlet in early August ($\delta^{18}O$ between −16.13 and −14.31 ‰) are enriched compared to the higher elevation road samples, show a great deal of variability despite having been obtained at a relatively close distance from each other and align at a slope of 6.50. The relative decrease in $\delta^{18}O$ associated with this slope is consistent with evaporation from the snowpack, a hypothesis further strengthened by the series of days with above 0 °C temperatures during July observed in the nearby 'Hornitos' meteorological station (Figure 2a).

The streamflow samples taken at the snout of the Juncal Norte glacier cluster together, despite the fact that they were measured throughout the entire melt season; the same is observed for the Mono-R1 samples. The range of variation in $\delta^{18}O$ in these glacial stream samples, from −19 to −17‰, is equivalent to approximately 10% of the beginning-of-spring value, which is larger, but in the order of, overall enrichment amounts reported by Taylor *et al*. (2002) for a series of catchments in maritime and continental climates. The larger range could be attributed to the higher evaporation and sublimation rates expected in the semi-arid Andes compared to those of other climates (Favier *et al*., 2009), which could lead to faster fractionation than that expected from melt alone. Still, this range of variation is very modest compared to the spatial variability observed in snow samples along the elevation gradient (road) at the end of winter. A similar result was documented recently by Penna *et al*. (2014), who describe a similar end-member behaviour in which glacier melt samples obtained at the ice surface show much lower variability than snowmelt samples.

Last, the isotopic composition of creek waters varies strongly depending on the sampling site location. The side-R1, 2 and 3 samples (obtained between November and March) are more depleted than the melt samples obtained in September in the lower part of the catchment. The slope of these samples in the isotopic line is roughly 4.0, lower than the slope value of the snow core samples taken at the beginning of spring near the basin outlet, and very similar to the slope of melt waters reported by Zhou *et al*. (2008a, b). The source of these waters must be snowmelt. Because isotopic fractionation in soil waters occurs at a very slow rate (Clark and Fritz, 1997), we can infer that the isotopic composition of these streams must be similar to the melt that fed them, which from snow cover imagery we can suppose occurred between September and November, 2011.

Hydrograph separation

Source determination. The biplot shown in Figure 5 displays the projection of each tracer data over the two-dimensional space determined by the dominant eigenvectors from principal component analysis (PCA). Principal components U1 and U2 explain 52% and 42% of the observed variance in Junc-R1 data, respectively, for a cumulative variance explanation of 94% in the two-dimensional reduced space (Table II). It can be seen that solutes and isotopes cluster together along two different directions, with isotopes more correlated with U2 and solutes having a larger projection along the U1 direction. Also, among solutes, sulphate and calcium are strongly correlated, whereas silica and magnesium move more towards U2 and potassium is almost orthogonal to isotope data. Based on the above, and on the fact that sulphate and calcium are the solutes displaying the largest

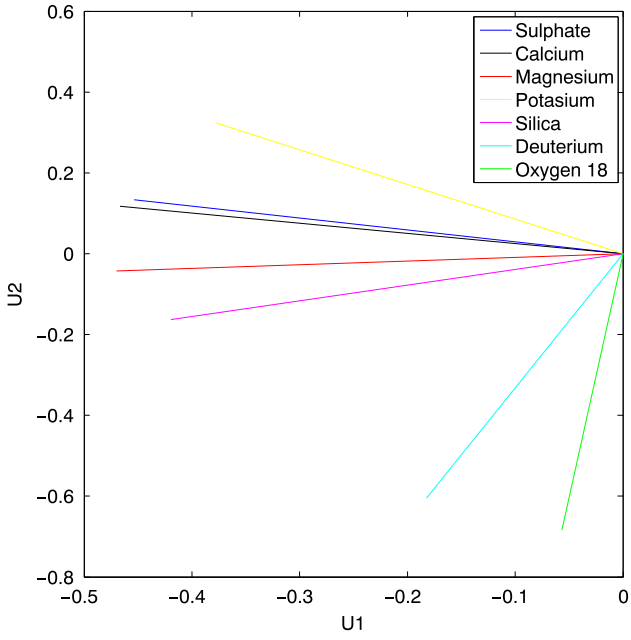

Figure 5. Biplot of tracer data at the Junc-R1 sampling site. Lines represent the projection of each tracer's data onto the reduced two-dimensional space formed by the two eigenvectors capturing the largest percentage of data variability

Table II. Summary of PCA results.

	First	Second	Third
Cumm. variance	52%	94%	99%
Eigenvalue	52%	41%	6%
Ca	−0.62	0.31	−0.08
SO^{4-}	−0.63	0.30	−0.16
δD	−0.41	−0.57	0.71
δ18O	−0.21	−0.70	−0.68

differences in concentration when comparing water samples taken at different locations in the basin, we retain sulphate, calcium and both stable isotopes as tracers for hydrograph separation.

Figure 6 shows the projection of water sample data on the reduced space determined by PCA utilizing sulphate, calcium and both stable isotopes. In this figure, Junc-R1 data is grouped in time according to the characteristic periods suggested by snow cover evolution from MODIS imagery. It can be seen that Junc-R1 is appropriately encircled by data obtained at side creeks (Side-R1, 2 and 3), at the Glac-R1 site (green stars) and at the eastern sub-basin outlets (Nava-R1 and Mono-R1). In an n-dimensional space, $n+1$ end-members are required for hydrograph separation. Our data is not sufficient for discriminating a fourth end-member, so a level of uncertainty remains with respect to the relative contribution of the Nava-R1 and Mono-R1 basins, which are separated in the plot because of small differences in isotopic signal and ion concentration. This uncertainty is explored in further detail in the next section, on hydrograph separation. Two samples obtained at a spring within the Navarro Creek basin (Nava-S1) show an even more extreme position in the reduced space. However, because these samples were obtained only at the end of the water year, we lack information on their temporal variability and decide to exclude them from the hydrograph separation analysis. Overall, isotopic signals attributable to liquid precipitation may be observed in our database. However, these inputs do not seem to contribute significantly to the melt season river volume, based on the joint inspection of tracer and river flow time series. The above analysis assumes that isotopic fractionation resulting from evaporation of soil and stream water is negligible with respect to other physical processes such as evaporation from the snowpack and altitudinal variation in isotopic signal because of temperature differences during precipitation events.

The information collected and presented above affords a plausible view of the geographical pathways of water as it moved through the basin during the 2011 water year. This conceptual model is shown in Figure 7. The western portion of the basin, associated with generally lower elevations and a predominantly volcanic geology, is associated with water samples that are isotopically enriched and low in calcium ions. Somewhat counterintuitively, water samples from this area are also low in sulphate concentrations. Water samples from this area align at a lower slope on the δD vs. $\delta^{18}O$ graph, evidencing also the influence of isotopic fractionation because of evaporation from the snowpack. The eastern portion of the basin is characterized by water samples with much higher (one order of magnitude) sulphate and calcium concentrations. These relate well with a more predominant influence of marine sedimentary deposits, volcanic rocks and with the presence of a few rock glaciers within the sub-catchment upstream of the Nava-R1 sampling site, more specifically near the sites Nava-S1 and Nava-S2 (Figure 1). At the same time, water samples from this eastern portion of the basin display a more depleted isotopic signal, coherent with the higher topographic elevations of snow accumulation and with a weaker influence of isotopic fractionation because of evaporation. Finally, water samples obtained at the Juncal Norte Glacier terminus (Glac-R1) show both very low concentration in all ions, and an isotopic signal almost equally depleted as that of the eastern portion of the basin. Based on this analysis, we propose the subdivision of the study basin in EAST, WEST and SOUTH sub-catchments or zones. The EAST zone is represented of the combination of waters sampled at locations Nava-R1 and Mono-R1, whereas the WEST zone is represented by

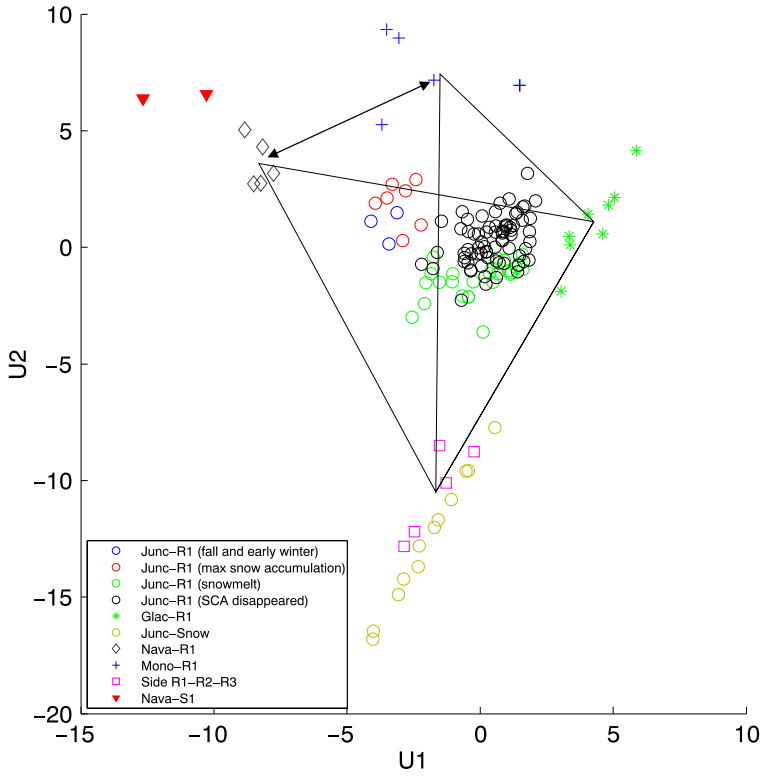

Figure 6. 2D mixing Uspace. Junc-R1 (basin outlet) data is presented in circles. Blue circles correspond to the beginning of the water year, in fall and early winter. Red circles correspond to winter (max. snow accumulation) season, green circles to spring (snow melt) season and finally black circles represent data obtained after snow covered disappeared almost completely from the basin and until the end of the water year, in April 2012. Junc-R1 samples are located in the interior space defined by combinations of the end-member samples such as side creeks, glacier subcatchment and major tributaries Navarro Creek (Nava-R1) and Mono de Agua Creek (Mono-R1). Double-ended arrow illustrates uncertainty in end-member best representing contribution from depleted isotopic and highly concentrated solute sources (Nava-R1 and Mono-R1)

the average of samples obtained at sites Side-R1, R2 and R3. Finally, the SOUTH zone is solely represented by water samples obtained at the Glac-R1 location. This conceptual model allows us to, via hydrograph separation, isolate the contribution of the glaciarized subcatchment containing the Juncal Norte Glacier. Because of the spatial configuration of this subcatchment, we expect that the vast majority of runoff coming from this basin originated from snow and ice melt, and that a large fraction of this melt occured over the surface of the Juncal Norte Glacier itself.

Juncal Norte glacier basin contribution to the 2011/2012 water year. Table III displays a summary of the results of all separation models to the water year hydrograph for the Juncal River Basin (Junc-R1). In order to account for the uncertainty regarding the relative contribution of the Navarro (Nava-R1) and Mono de Agua (Mono-R1) sub-catchments we ran three separation scenarios. On the extremes, we supposed that either the Nava-R1 contributes the entirety of the EAST sub-region or that Mono-R1 is the area contributing all of the runoff. In between these two unrealistic cases, we suppose that the relative contribution is proportional to the surface area of each sub-basin, such that the Navarro and Mono de Agua Creeks contribute 59 and 41% of flow from the EAST zone, respectively. Results are presented for four sub-periods as a function of snow cover dynamics derived from MODIS data.

Focusing the analysis on the contribution of the SOUTH sub-basin, we see that a plausible scenario results in water yields from this sub-catchment that increase monotonically from 14% in the fall season to 49% in summer. According to this separation, contribution in winter is non-negligible, but is dwarfed by the relative participation between October and March. The WEST portion of the basin contributes rather evenly (23 to 31%) to flow during the year, which could be attributed to autumn precipitation either running off or melting quickly from low elevation areas. The largest contribution to overall flow during fall and winter (61–63%) is attributed to the EAST sub-region. This can be interpreted as an indication of water storage from the previous water year: during the period in which EAST contributes most significantly (April through September), basin wide snow cover is either increasing or flat, which suggests that little snow should be melting at this time.

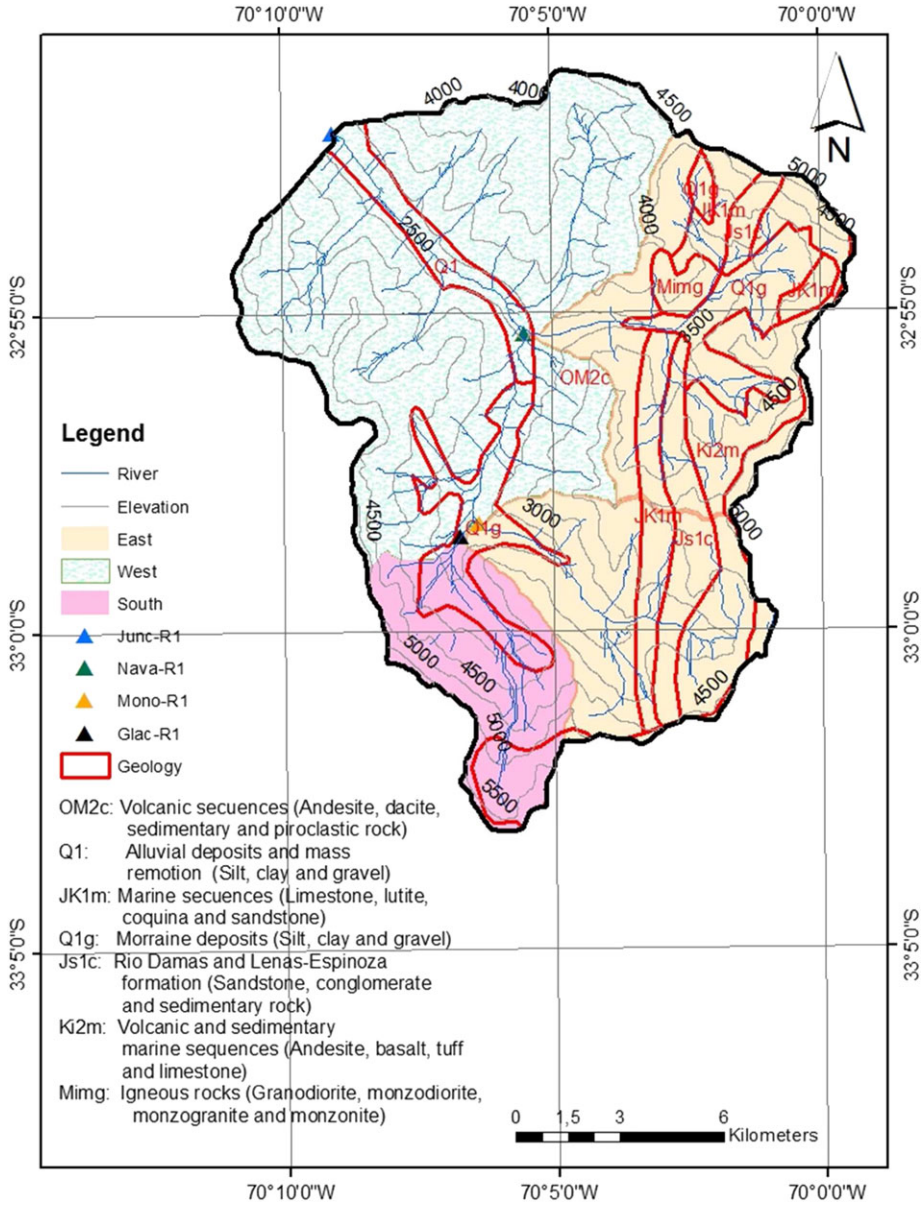

Figure 7. Conceptual tracer-based geographical basin subdivision, showing elevation contours, geological features, river network and hydrological units 'East', 'West' and 'South'. 'East' is characterized as a combination of the tracer signatures measured at Nava-R1 and Mono-R1. 'West' is characterized by the tracer signature measured at Side-R1, 2 and 3. 'South' denotes the sub-catchment containing the Juncal Norte Glacier

Averaged values over periods of time offer only a partial picture of the complexity of river behaviour. Figure 8 shows the hydrograph separation results as a time series: the upper panel presents absolute streamflow values whereas the lower panel presents percentage values. In this plot, we include only the more realistic case in which the Navarro Creek (Nava-R1) and Mono de Agua (Mono-R1) sub-catchments contribute to runoff proportionally to their surface area. Overall, the highest contribution from the SOUTH sub-basin in absolute terms occurs by the end of December 2011, with an approximate absolute value of $5\,m^3\,s^{-1}$. After that, the outflow from this area decreases slowly to approximately $2\,m^3\,s^{-1}$. Our data is insufficient to diagnose the hydrologic features determining these patterns, but the sequential disappearance of accumulated seasonal snowpack from the SOUTH sub-basin and short hydrologic transit times within this steep, rocky catchment may explain this variability. Future research should be aimed at contrasting these temporal variability patterns with physically based modelling approximations of the basin, in order to test the plausibility and relative importance of different hydrologic processes in determining streamflow behaviour.

Table III. Summary of relative source contribution estimation. Values are fractions contributed by each subcatchment to flow observed at the Junc-R1 sampling site. In parenthesis, lower and upper 95% confidence limits from the posterior distribution obtained from the MCMC solution to the Bayes equation. Values of 'f' parameter indicate alternative scenarios of the relative contribution of the Nava-R1 subcatchment to the 'EAST' zone. f = 1 and 0 are non-realistic extreme values, and f = 0.41 is based on the Nava-R1 surface-area contribution to the 'EAST' zone. Rows indicate subperiods defined on the basis of snow-cover evolution.

	f = 1 (All from Navarro Creek)				f = 0 (All from Mono de Agua Creek)				f = 0.41 (Area-based distribution)			
SCA dates	WEST	EAST	SOUTH	Total	WEST	EAST	SOUTH	Total	WEST	EAST	SOUTH	Total
30/04/11 – 04/08/11	0.13	0.55	0.32	1.00	0.30	0.60	0.10	1.00	0.21	0.64	0.15	1.00
	(0.03– 0.25)	(0.45– 0.64)	(0.22– 0.41)		(0.19– 0.42)	(0.47– 0.72)	(0.01– 0.25)		(0.08– 0.34)	(0.51– 0.80)	(0.02– 0.30)	
11/08/11 – 21/09/11	0.12	0.50	0.38	1.00	0.30	0.58	0.12	1.00	0.20	0.60	0.20	1.00
	(0.03– 0.25)	(0.40– 0.58)	(0.28– 0.47)		(0.19– 0.43)	(0.44– 0.71)	(0.01– 0.29)		(0.08– 0.33)	(0.46– 0.75)	(0.04– 0.36)	
05/10/11 – 25/11/11	0.27	0.19	0.54	1.00	0.39	0.29	0.31	1.00	0.31	0.23	0.46	1.00
	(0.10– 0.45)	(0.07– 0.30)	(0.40– 0.69)		(0.24– 0.55)	(0.11– 0.49)	(0.07– 0.54)		(0.15– 0.47)	(0.09– 0.37)	(0.30– 0.63)	
26/11/11 – 31/03/12	0.16	0.22	0.62	1.00	0.30	0.37	0.34	1.00	0.20	0.27	0.53	1.00
	(0.04– 0.32)	(0.10– 0.33)	(0.49– 0.76)		(0.15– 0.45)	(0.16– 0.58)	(0.06– 0.60)		(0.06– 0.35)	(0.12– 0.42)	(0.37– 0.70)	

Expressing the above estimates in terms of contributions of *geographical* sources rather than *hydrologic-type* sources, such as snowmelt, ice melt or groundwater, is necessary because of the lack of direct measurements of these types of hydrological stores and therefore is required to alleviate this important source of uncertainty. Indeed, previous exercises in hydrograph separation in mountainous watersheds (e.g. Cable *et al*., 2011; Penna *et al*., 2014; Taylor *et al*., 2002) have been able to more directly characterize end-members by sampling glacier ice, snowmelt through snow lysimeters or groundwater from wells. Limitations in our experimental setup prevented us from achieving this (Rodriguez *et al*., 2014). However, of the three identified sources used in hydrograph separation, two – EAST and SOUTH – were derived after analysing several water samples collected at regular intervals during the water year. The tracer information from these samples showed some variability, but no identifiable trends during the study period. This stability in time is an important condition for hydrograph separation and gives further confidence in our results. The remaining source, namely WEST, was derived from fewer water samples obtained later in the water year, approximately at the beginning and end of summer, when snow had disappeared from that portion of the basin. Therefore, this source is affected by greater uncertainty, not quantifiable with our data, because its isotopic signal at earlier dates (in particular during winter and spring) might have been less affected by sublimation and evaporation. Nevertheless, the fact that these data points lie very near the 'snow-road' samples, which were obtained much earlier in the season (August 2011), and away from Glac-R1 and Mono-R1/Nava-R1 samples in the reduced space (Figure 6) lends credibility to the hypothesis that this geographical source is indeed identifiable and appropriately represented by these water samples.

We argue here that differences in hydrologic contribution from the three identified zones are mainly derived from the disproportionate distribution of ice masses throughout the basin. Other hydrologic features that exhibit spatial variability include precipitation, which is mainly subject to an elevation gradient because of orographic uplifting (Ragettli *et al*., 2014). Vegetation cover is very sparse and limited to restricted areas on the alluvial fill next to river channels. Orographic precipitation patterns could explain runoff yield differences between low-lying areas, which are preferably concentrated in the 'WEST' zone, and higher ground. But the 'EAST' and 'SOUTH' zones show a similar elevation distribution. Furthermore, the 'SOUTH' zone has a much smaller surface area, yet its contribution is significantly larger during spring and summer months (Table III). Spatial differences in precipitation are very unlikely to explain this variability. The fact that no rain gages or

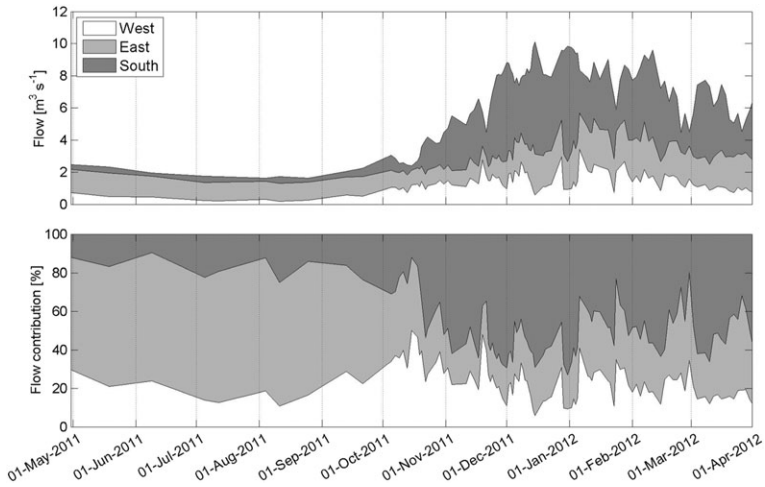

Figure 8. Hydrograph separation at the Juncal en Juncal river basin (Junc-R1) for the 2011/2012 water year. Upper panel shows absolute values; lower panel shows relative fractions for each geographical source

snow accumulation sensors existed within the basin exacerbates this source of uncertainty, which remains an area of future research in this region.

During 2011/2012, the Juncal river watershed experienced very dry conditions, with annual flow on the 8th decile and with winter precipitation measured at the Riecillos rain gage having a probability of exceedance of 83%. For these conditions, our results suggest that the SOUTH sub-basin contributed approximately one half of all river flow volume measured at the Junc-R1 site during the melt season, despite representing only 11% of the total catchment area. The sub-sector of the basin more strongly associated with rock-water interaction (EAST) contributed with 60% of all river flow during the fall and winter seasons, an unexpected result hinting at the importance of subsurface storage in mountainous catchments. An alternative hypothesis would attribute a significant portion of flow from the EAST zone to rock glacier contribution, because water samples obtained at the Nava-S1 and Nava-S2 sites were very similar in tracer signature to those at the Nava-R1 site. Williams *et al.* (2006) observed very high concentrations of calcium, sulphate and other solutes in water samples seeping from rock glaciers in the Colorado Front Range, and concluded that these ice bodies where the main sources of base flow. In the Andes, recent research has pointed at the hydrological relevance of rock glaciers (e.g. Azócar and Brenning, 2010; Brenning, 2005). Future work should strive at characterizing the behaviour of these water stores through novel data such as demonstrated by Langston *et al.* (2013).

The estimated contribution originating from the SOUTH zone under the baseline simulation averages $3.4\,m^3\,s^{-1}$ (95% confidence interval is $2.4 - 4.6\,m^3\,s^{-1}$) at the Juncal river Basin outlet between September 2011 and April 2012. This basin is a tributary to the Aconcagua River at the *Chacabuquito* streamgage, which has a contributing area of $2400\,km^2$. During the 2011/2012 melt season, the average SEP-APR river flow observed at that location was $16\,m^3\,s^{-1}$. In other words, the 27-km^2 SOUTH sub-basin, represented approximately 20% (95% range of 15 – 28%) of melt season flow measured at the Chacabuquito gage. When considering only the January – April period, the SOUTH contribution is $3.6\,m^3\,s^{-1}$ (95% range of $2.4 - 4.8\,m^3\,s^{-1}$) out of $19.7\,m^3\,s^{-1}$, or 18% (95% range of 12 – 24%). The fact that the 27-km^2 glacierized sub-catchment containing a 9-km^2 glacier might contribute in the order of a fifth of all river flow for the larger Aconcagua at Chacabuquito river basin highlights the need for continued research and greater understanding of the role and future evolution of the Andes cryosphere with respect to water resources.

CONCLUSION

This study documents a hydrograph separation exercise aimed at estimating the hydrological role of glaciers in a high elevation, Andean watershed in Central Chile during a dry water year (2011/2012). Water isotopic and chemical characteristics were sampled at high temporal resolution at the basin outlet, and these observations were complemented with information from synoptic measurements at several locations within the basin, each representing a distinct hydrological feature.

This research demonstrates the capability of combined isotopic and solute information for informing mixing models for hydrologic research in mountain environments. We were successful in capturing and uncovering relevant modes of variability of the problem by rotating the system of reference and reducing the variation space to at most three directions, using PCA. A Bayesian version of a mixing model provided uncertainty bounds

on the relative importance of each source, and it was found that collected data from the 2011/2012 water year narrowed the expected error of our estimates from that expected from the prior estimates based on recent literature. Based on our geographical source analysis, we were able to identify and quantify three different sources of flow in the basin, namely SOUTH, strongly related to glacier presence and low ion concentrations; WEST, associated to quick-flowing snowmelt; and EAST, related to high ion concentrations proper to high rock-water interaction and a depleted isotopic signal proper of high-elevation accumulation zones. Our experimental design does not enable the assessment of time-varying isotopic composition of snow and glacier melt because of isotopic fractionation, so we were unable to discriminate between different types of sources, specially between seasonal snowpack and glacier melt. However, we are able to provide fairly reliable estimates of the contribution of a specific sub-catchment that is strongly determined by the presence of a clean glacier covering a significant fraction of its surface area. Because our data covers one water year only, we are not able to discuss interannual variability or its governing processes at this time. This is relevant, because it may be expected that relative contributions of storage compartments such as glaciers and groundwater could depend on antecedent conditions at yearly time scales. Future research should explore these effects further, particularly in this and other regions with important hydroclimatic variability.

Future field designs in this region should sample directly the ice surface, in order to obtain isotopic characteristics associated with superficial ice-cores, firn and on-glacier snow. Also, the altitudinal variation in isotopic snow properties was sampled at a rather limited range, and higher elevation snow properties may suggest different interpretation of isotopic flow characteristics. Together with uncertainty on the influence of fractionation processes and preferential elution on the geochemical characteristics, these aspects constitute avenues for further improvement of our models. Finally, we were unable to obtain direct samples of subsurface water. Future experiments should consider wells dug in valley bottoms and analysis of other element isotopes sensitive to water-soil interaction, which would allow for an integrated view of the subsurface behaviour of relevant aquifer systems in mountain catchments, in terms of isotopic, chemical and hydrologic variables.

AUTHOR CONTRIBUTION

F. Pellicciotti and J. McPhee acted as project leaders. N. Ohlanders, F. Pellicciotti and M. Rodriguez designed the field experiments, while N. Ohlanders and M. Rodriguez led the data collection campaigns. M. Rodriguez developed the analysis methodology and carried out the bulk of the presented calculations. Finally, J. McPhee and M. Rodriguez shared responsibility in manuscript preparation with significant feedback from N. Ohlanders, M. Williams and F. Pellicciotti.

ACKNOWLEDGEMENTS

This research was funded by CONICYT under grants SER-003 and FONDECYT-1121184. The authors thank Katja Deckart and Amparo Edwards for their insightful comments on this work, and Viviana Lorca for her invaluable laboratory assistance. Thanks also to Edward Cornwell, Sebastian Krögh, Braulio Salgado, Simone Schauwecker and Alvaro Ayala for their assistance during field data collection. Finally, we are very grateful to Catherine Kenrick and to 'Parque Andino Juncal', for granting access and providing logistical assistance during field campaigns.

REFERENCE

Azócar GF, Brenning A. 2010. Hydrological and geomorphological significance of rock glaciers in the dry Andes, Chile (27–33 S). *Permafr. Periglac. Process.* **21**(1): 42–53.

Baraer M, McKenzie JM, Mark BG, Bury J, Knox S. Characterizing contributions of glacier melt and groundwater during the dry season in a poorly gauged catchment of the Cordillera Blanca (Peru), [online] Available from: https://kb.osu.edu/dspace/handle/1811/49183 (Accessed 16 April 2016), 2009.

Baraer M, Mark B, McKenzie J, Condom T, Bury J, Huh K-I, Portocarrero C, Gomez J, Rathay S. 2012. Glacier recession and water resources in Peru's Cordillera Blanca. *J. Glaciol.* **58**(207): 134–150. DOI:10.3189/2012JoG11J186

Barthold FK, Tyralla C, Schneider K, Vaché KB, Frede H-G, Breuer L. 2011. How many tracers do we need for end member mixing analysis (EMMA)? A sensitivity analysis. *Water Resour. Res.* **47**(8): W08519–W08519. DOI:10.1029/2011WR010604

Bown F, Rivera A, Acuña C. 2008. Recent glacier variations at the Aconcagua basin, central Chilean Andes. *Ann. Glaciol.* **48**(1): 43–48. DOI:10.3189/172756408784700572

Brenning A. 2005. Geomorphological, hydrological and climatic significance of rock glaciers in the Andes of Central Chile (33–35 S). *Permafr. Periglac. Process.* **16**(3): 231–240.

Cable J, Ogle K, Williams D. 2011. Contribution of glacier meltwater to streamflow in the Wind River Range, Wyoming, inferred via a Bayesian mixing model applied to isotopic measurements. *Hydrol. Process.* **25**(14): 2228–2236. DOI:10.1002/hyp.7982

Casassa G, Espizua LE, Francou B, Ribstein P, Ames A, Alean J. 1998. In *Glaciers in South America, in Into the second century of worldwide glacier monitoring: prospects and strategies*, Haeberli W, Hoelzle M, Suter S (eds). United Nations Publications: Paris; 125–146.

Christophersen N, Hooper RP. 1992. Multivariate analysis of stream water chemical data: the use of principal components analysis for the end-member mixing problem. *Water Resour. Res.* **28**(1): 99–107.

Christophersen N, Neal C, Hooper RP, Vogt RD, Andersen S. 1990. Modelling streamwater chemistry as a mixture of soilwater end-members—a step towards second-generation acidification models. *J. Hydrol.* **116**(1): 307–320.

Clark I, Fritz P. 1997. *Environmental isotopes in hydrogeology*, 2nd edition. Lewis Publishers: New York, USA.

Craig H. 1961. Isotopic variations in meteoric waters. *Science* **133**(3465): 1702–3. DOI:10.1126/science.133.3465.1702

Dirección Meteorológica de Chile Publications. Climatología regional, [online] Available from: http://www.meteochile.gob.cl/climatologia.php, 2001.

Favier V, Falvey M, Rabatel A, Praderio E, López D. 2009. Interpreting discrepancies between discharge and precipitation in high-altitude area of Chile's Norte Chico region (26–32°S). *Water Resour. Res.* **45**(2): W02424. DOI:10.1029/2008WR006802

Freer J, Beven K, Ambroise B. 1996. Bayesian estimation of uncertainty in runoff prediction and the value of data: an application of the GLUE approach. *Water Resour. Res.* **32**(7): 2161–2173.

Gascoin S, Kinnard C, Ponce R, Lhermitte S, MacDonell S, Rabatel A. 2011. Glacier contribution to streamflow in two headwaters of the Huasco River, Dry Andes of Chile. *The Cryosphere* **5**(4): 1099–1113. DOI:10.5194/tc-5-1099-2011

Gordon RP, Lautz LK, McKenzie JM, Mark BG, Chavez D, Baraer M. 2015. Sources and pathways of stream generation in tropical proglacial valleys of the Cordillera Blanca, Peru. *J. Hydrol.* **522**: 628–644. DOI:10.1016/j.jhydrol.2015.01.013

Hannah DM, Gurnell AM. 2001. A conceptual, linear reservoir runoff model to investigate melt season changes in cirque glacier hydrology. *J. Hydrol.* **246**(1-4): 123–141. DOI:10.1016/S0022-1694(01)00364-X

Heppell CM, Chapman a S. 2006. Analysis of a two-component hydrograph separation model to predict herbicide runoff in drained soils. *Agric Water Manag* **79**(2): 177–207. DOI:10.1016/j.agwat.2005.02.008

Hirabayashi Y, Döll P, Kanae S. 2010. Global-scale modeling of glacier mass balances for water resources assessments: glacier mass changes between 1948 and 2006. *J. Hydrol.* **390**(3-4): 245–256. DOI:10.1016/j.jhydrol.2010.07.001

Hodgkins R. 1997. Glacier hydrology in Svalbard, Norwegian high arctic. *Quat. Sci. Rev.* **16**(97): 957–973.

Jansson P, Hock R, Schneider T. 2003. The concept of glacier storage: a review. *J. Hydrol.* **282**(1-4): 116–129. DOI:10.1016/S0022-1694(03)00258-0

Johannessen M, Henriksen A. 1978. Chemistry of snow meltwater: changes in concentration during melting. *Water Resour. Res.* **14**(4): 615–619. DOI:10.1029/WR014i004p00615

Kaser G, Juen I, Georges C, Gómez J, Tamayo W. 2003. The impact of glaciers on the runoff and the reconstruction of mass balance history from hydrological data in the tropical Cordillera Blanca, Perú. *J. Hydrol.* **282**(1-4): 130–144. DOI:10.1016/S0022-1694(03)00259-2

Kirchner JW. 2003. A double paradox in catchment hydrology and geochemistry. *Hydrol. Process.* **17**(4): 871–874. DOI:10.1002/hyp.5108

Klaus J, McDonnell JJ. 2013. Hydrograph separation using stable isotopes: review and evaluation. *J. Hydrol.* **505**: 47–64. DOI:10.1016/j.jhydrol.2013.09.006

Ladouche B, Probst A, Viville D, Idir S, Baqué D, Loubet M, Probst J-L, Bariac T. 2001. Hydrograph separation using isotopic, chemical and hydrological approaches (Strengbach catchment, France). *J. Hydrol.* **242**(3–4): 255–274. DOI:10.1016/S0022-1694(00)00391-7

Langston G, Hayashi M, Roy JW. 2013. Quantifying groundwater–surface water interactions in a proglacial moraine using heat and solute tracers. *Water Resour. Res.* **49**(9): 5411–5426.

Laudon H, Slaymaker O. 1997. Hydrograph separation using stable isotopes, silica and electrical conductivity: an alpine example. *J. Hydrol.* **201**(1-4): 82–101. DOI:10.1016/S0022-1694(97)00030-9

Liu F, Williams MW, Caine N. 2004. Source waters and flow paths in an alpine catchment, Colorado Front Range, United States. *Water Resour. Res.* **40**: 1–16. DOI:10.1029/2004WR003076

Liu Y, Gupta HV. 2007. Uncertainty in hydrologic modeling: toward an integrated data assimilation framework, *Water Resour. Res.*, **43**(7) [online] Available from: http://onlinelibrary.wiley.com/doi/10.1029/2006WR005756/full (Accessed 16 April 2016).

Liu Y, Fan N, An S, Bai X, Liu F, Xu Z, Wang Z, Liu S. 2008. Characteristics of water isotopes and hydrograph separation during the wet season in the Heishui River, China. *J. Hydrol.* **353**(3-4): 314–321. DOI:10.1016/j.jhydrol.2008.02.017

Marengo JA, Pabón JD, Díaz A, Rosas G, Ávalos G, Montealegre E, Villacis M, Solman S, Rojas M. 2011. Climate change: evidence and future scenarios for the Andean region, in climate change and biodiversity in the tropical Andes. In *Inter-American Institute for Global Change Research (IAI) and Scientific Committee on Problems of the Environment (SCOPE)*, Herzog SK, Martínez R, Jørgensen PM, Tiessen H (eds). Paris; 110–127.

McPhee J, Cortés G, Rojas M, Garcia L, Descalzi A, Vargas L. Downscaling climate changes for Santiago: what effects can be expected? In *Climate adaptation Santiago*, edited by K. Krellenberg and B. Hansjürgens, pp. 19–41, Springer Berlin Heidelberg. [online] Available from: http://link.springer.com/chapter/10.1007/978-3-642-39103-3_2 (Accessed 1 October 2014), 2014.

Meriano M, Howard KWF, Eyles N. 2011. The role of midsummer urban aquifer recharge in stormflow generation using isotopic and chemical hydrograph separation techniques. *J. Hydrol.* **396**(1-2): 82–93. DOI:10.1016/j.jhydrol.2010.10.041

Merot P, Durand P, Morisson C. 1995. Four-component hydrograph separation using isotopic and chemical determinations in an agricultural catchment in western France. *Phys. Chem. Earth* **20**(3-4): 415–425. DOI:10.1016/0079-1946(95)00055-0

Mingjie G, Tianding H, Baisheng Y, Keqin J. 2013. Characteristics of melt water discharge in the Glacier No. 1 basin, headwater of Urumqi River. *J. Hydrol.* **489**(1): 180–188. DOI:10.1016/j.jhydrol.2013.03.013

Moore JW, Semmens BX. 2008. Incorporating uncertainty and prior information into stable isotope mixing models. *Ecol. Lett.* **11**(5): 470–80. DOI:10.1111/j.1461-0248.2008.01163.x

Mul M, Mutiibwa R, Uhlenbrook S, Savenije H. 2008. Hydrograph separation using hydrochemical tracers in the Makanya catchment, Tanzania. *Phys. Chem. Earth Parts ABC* **33**(1-2): 151–156. DOI:10.1016/j.pce.2007.04.015

Neal C. 2001. Alkalinity measurements within natural waters: towards a standardised approach. *Sci. Total Environ.* **265**(1–3): 99–113.

Ogunkoya O, Jenkins A. 1993. Analysis of storm hydrograph and flow pathway using a three-component hydrograph separation model. *J. Hydrol.* **142**: 71–88.

Ohlanders N, Rodriguez M, McPhee J. 2013. Stable water isotope variation in a Central Andean watershed dominated by glacier and snowmelt. [online] Available from: http://www.hydrol-earth-syst-sci.net/17/1035/2013/hess-17-1035-2013.pdf (Accessed 1 October 2014).

Parnell AC, Inger R, Bearhop S, Jackson AL. 2010. Source partitioning using stable isotopes: coping with too much variation. *PLoS One* **5**(3): e9672–e9672. DOI:10.1371/journal.pone.0009672

Pellicciotti F, Helbing J, Rivera A, Favier V, Corripio J, Araos J, Sicart J-E, Carenzo M. 2008. A study of the energy balance and melt regime on Juncal Norte Glacier, semi-arid Andes of central Chile, using melt models of different complexity. *Hydrol. Process.* **22**(19): 3980–3997. DOI:10.1002/hyp.7085

Pellicciotti F, Ragettli S, Carenzo M, McPhee J. 2014. Changes of glaciers in the Andes of Chile and priorities for future work. *Sci. Total Environ.* **493**: 1197–1210. DOI:10.1016/j.scitotenv.2013.10.055

Peña H, Nazarala B. 1987. In *Snowmelt-runoff simulation model of a central Chile Andean basin with relevant orographic effect, in Large Scale Effects of Seasonal Snow Cover*, Goodison BE, Barry RG, Dozier J (eds), **166**. IAHS Publ: Vancouver, Canada; 161–172.

Penna D, Engel M, Mao L, Dell'Agnese A, Bertoldi G, Comiti F. 2014. Tracer-based analysis of spatial and temporal variations of water sources in a glacierized catchment. *Hydrol. Earth Syst. Sci.* **18**(12): 5271–5288. DOI:10.5194/hess-18-5271-2014

Ragettli S, Pellicciotti F. 2012. Calibration of a physically based, spatially distributed hydrological model in a glacierized basin: on the use of knowledge from glaciometeorological processes to constrain model parameters. *Water Resour. Res.* **48**(3): W03509–W03509. DOI:10.1029/2011WR010559

Ragettli S, Cortés G, McPhee J, Pellicciotti F. 2014. An evaluation of approaches for modelling hydrological processes in high-elevation, glacierized Andean watersheds. *Hydrol. Process.* **28**(23): 5674–5695. DOI:10.1002/hyp.10055

Rodriguez M, Ohlanders N, McPhee J. 2014. Estimating glacier and snowmelt contributions to stream flow in a Central Andes catchment in Chile using natural tracers. *Hydrol Earth Syst Sci Discuss* **11**(7): 8949–8994. DOI:10.5194/hessd-11-8949-2014

Semmens BX, Ward EJ, Moore JW, Darimont CT. 2009. Quantifying inter- and intra-population niche variability using hierarchical bayesian stable isotope mixing models. *PLoS One* **4**(7): e6187–e6187. DOI:10.1371/journal.pone.0006187

SERNAGEOMIN. 2002. Geological map of Chile, [online] Available from: http://tienda.sernageomin.cl/TiendaVirtual/ProductDetail.aspx?pid=1949 (Accessed 3 January 2015).

Singh P, Haritashya UK, Kumar N, Singh Y. 2006. Hydrological characteristics of the Gangotri Glacier, central Himalayas, India. *J. Hydrol.* **327**(1-2): 55–67. DOI:10.1016/j.jhydrol.2005.11.060

Soulsby C, Dunn SM. 2003. Towards integrating tracer studies in conceptual rainfall–runoff models: recent insights from a sub-arctic catchment in the Cairngorm Mountains, Scotland. *Hydrol. Process.* **17**(2): 403–416. DOI:10.1002/hyp.1132

Steyvers M. 2011. *Computational statistics with Matlab*. Lecture, University of California Irvine: Irvine, CA, USA.

Taylor S, Feng X, Williams M, McNamara J. 2002. How isotopic fractionation of snowmelt affects hydrograph separation. *Hydrol. Process.* **16**(18): 3683–3690. DOI:10.1002/hyp.1232

Thadewald T, Büning H. 2007. Jarque–Bera test and its competitors for testing normality—a power comparison. *J. Appl. Stat.* **34**(1): 87–105.

Verbunt M, Gurtz J, Jasper K, Lang H, Warmerdam P, Zappa M. 2003. The hydrological role of snow and glaciers in alpine river basins and their distributed modeling. *J. Hydrol.* **282**(1-4): 36–55. DOI:10.1016/S0022-1694(03)00251-8

Wagnon P, Ribstein P, Kaser G, Berton P. 1999. Energy balance and runoff seasonality of a Bolivian glacier. *Glob. Planet. Change* **22**(1-4): 49–58. DOI:10.1016/S0921-8181(99)00025-9

Wikle CK, Berliner LM. 2007. A Bayesian tutorial for data assimilation. *Phys. Nonlinear Phenom.* **230**(1-2): 1–16. DOI:10.1016/j.physd.2006.09.017

Williams DG, Cable J, Ogle K. 2009. Tracing glacial ice and snow meltwater with isotopes. 1–9.

Williams MW, Melack JM. 1991. Solute chemistry of snowmelt and runoff in an Alpine Basin, Sierra Nevada. *Water Resour. Res.* **27**(7): 1575–1588. DOI:10.1029/90WR02774

Williams MW, Knauf M, Caine N, Liu F, Verplanck PL. 2006. Geochemistry and source waters of rock glacier outflow, Colorado Front Range. *Permafr. Periglac. Process.* **17**(1): 13–33. DOI:10.1002/ppp.535

Yu W, Yao T, Kang S, Pu J, Yang W, Gao T, Zhao H, Zhou H, Li S, Wang W, Ma L. 2013. Different region climate regimes and topography affect the changes in area and mass balance of glaciers on the north and south slopes of the same glacierized massif (the West Nyainqentanglha Range, Tibetan Plateau). *J. Hydrol.* **495**: 64–73. DOI:10.1016/j.jhydrol.2013.04.034

Zhou S, Nakawo M, Hashimoto S, Sakai A. 2008a. Preferential exchange rate effect of isotopic fractionation in a melting snowpack. *Hydrol. Process.* **22**(18): 3734–3740. DOI:10.1002/hyp.6977

Zhou S, Nakawo M, Hashimoto S, Sakai A. 2008b. The effect of refreezing on the isotopic composition of melting snowpack. *Hydrol. Process.* **22**(6): 873–882. DOI:10.1002/hyp.6662

